bioRxiv preprint doi: https://doi.org/10.1101/2020.09.16.299883; this version posted September 17, 2020. The copyright holder for this preprint (which was not certified by peer review) is the author/funder, who has granted bioRxiv a license to display the preprint in perpetuity. It is made available under aCC-BY-NC-ND 4.0 International license.

Large-scale identification of ubiquitination sites on membrane-associated proteins in *Arabidopsis thaliana* seedlings

Lauren E. Grubb[1,2,+], Paul Derbyshire[2], Katherine Dunning[1], Cyril Zipfel[2,3], Frank L.H. Menke[2,*], and Jacqueline Monaghan[1,2,*]

[1]Department of Biology, Queen's University, Kingston, Canada
[2]The Sainsbury Laboratory, University of East Anglia, Norwich Research Park, Norwich, United Kingdom
[3]Department of Plant and Microbial Biology, Zurich-Basel Plant Science Center, University of Zurich, Zurich, Switzerland

[+]Current address: John Innes Centre, Norwich Research Park, Norwich, United Kingdom

*Corresponding authors: frank.menke@tsl.ac.uk
jacqueline.monaghan@queensu.ca

bioRxiv preprint doi: https://doi.org/10.1101/2020.09.16.299883; this version posted September 17, 2020. The copyright holder for this preprint (which was not certified by peer review) is the author/funder, who has granted bioRxiv a license to display the preprint in perpetuity. It is made available under aCC-BY-NC-ND 4.0 International license.

Abstract

Protein phosphorylation and ubiquitination are two of the most abundant forms of post-translational modifications in eukaryotes, regulated by thousands of protein kinases, phosphatases, E3 ubiquitin ligases, and ubiquitin proteases. Although previous studies have catalogued several ubiquitinated proteins in plants (Walton et al., 2016), few membrane-localized proteins have been identified. Receptor kinases (RKs) initiate phosphorylation signal relays that regulate plant growth, development, and stress responses. While the regulatory role of phosphorylation on protein kinase function is well-documented (Couto and Zipfel, 2016), considerably less is known about the role of ubiquitination on protein kinase function, even though protein turnover is critical to their signaling competence and cellular homeostasis. Here we describe the large-scale identification of ubiquitination sites on Arabidopsis proteins associated with or integral to the plasma membrane, including over 100 protein kinases.

Introduction

Proteins can be mono-, poly-, and/or multi-mono-ubiquitinated, each affecting protein function in different ways. For example, mono-ubiquitination is often associated with protein activation or endocytosis, whereas poly-ubiquitination is often a mark for proteasomal degradation (Vierstra, 2012; Paez Valencia et al., 2016). Dynamic interplay between phosphorylation and ubiquitination has been observed in several proteins involved in immune signaling (Mithoe and Menke, 2018), including layered post-translational regulation of the receptor-like cytoplasmic kinase (RLCK) BIK1. BIK1 is directly phosphorylated and activated by several ligand-bound RKs (Couto and Zipfel, 2016), and can be dephosphorylated by the phosphatase PP2C38 (Couto

bioRxiv preprint doi: https://doi.org/10.1101/2020.09.16.299883; this version posted September 17, 2020. The copyright holder for this preprint (which was not certified by peer review) is the author/funder, who has granted bioRxiv a license to display the preprint in perpetuity. It is made available under aCC-BY-NC-ND 4.0 International license.

et al., 2016). Precise control of BIK1 abundance is regulated by poly-ubiquitination by the E3 ligases PUB25 and PUB26 (Wang et al., 2018), as well as phosphorylation by the calcium-dependent protein kinase CPK28 (Monaghan et al., 2014; Wang et al., 2018) and the mitogen-activated protein kinase kinase kinase kinase (MAP4K) SIK1/MAP4K4 (Zhang et al., 2018; Jiang et al., 2019). Most recently, it was shown that BIK1 is also mono-ubiquitinated by the E3 ligases RHA3A and RHA3AB to regulate its activation and endocytosis (Ma et al., 2020).

Results and Discussion

Proteomics and mutagenesis approaches have resulted in the discovery of several phosphorylated residues on BIK1 (Liang and Zhou, 2018). To help us understand the role of ubiquitination on BIK1 function, we set out to identify *in vivo* ubiquitination sites on BIK1. We enriched for plasma membrane-localized BIK1 by isolating microsomal protein fractions from Col-0/*pBIK1:BIK1-HA*, *cpk28-1/pBIK1:BIK1-HA* and *CPK28-OE1/pBIK1:BIK1-HA* genotypes, which express 100-fold higher levels of *BIK1* and differentially accumulate BIK1 protein compared to wild-type (Monaghan et al., 2014). To increase protein abundance and allow us to potentially capture immune-induced ubiquitination, proteasomal machinery was inhibited with 50 μM MG-132 an hour before treatment with water or 1 μM elf18 (an immunogenic peptide derived from bacterial EF-Tu (Zipfel et al., 2006)). Microsomal protein fractions were digested with trypsin, and anti-K-ε-GG agarose beads (Udeshi et al., 2013) were used to enrich for ubiquitinated peptides by affinity binding. Ubiquitinated lysines were identified based on a shift of ~114 Da - the mass of two glycine remnants that remain covalently bound to lysines following trypsin digestion - using liquid chromatography followed by tandem mass spectrometry (LC-MS/MS) (Supplementary Methods).

bioRxiv preprint doi: https://doi.org/10.1101/2020.09.16.299883; this version posted September 17, 2020. The copyright holder for this preprint (which was not certified by peer review) is the author/funder, who has granted bioRxiv a license to display the preprint in perpetuity. It is made available under aCC-BY-NC-ND 4.0 International license.

We confidently identified a total of 916 ubiquitinated peptides on 450 proteins across several biological replicates with a peptide false discovery rate of 0.025 (Table S1), and an additional 526 peptides on 398 proteins observed in single experiments (Table S2). Included in these data were seven ubiquitinated lysines on BIK1 (Tables 1, S1, S2, and Figure 1). Given our particular interest in BIK1, we manually inspected all spectra mapping to BIK1 and found an additional three sites (Figures 1 and S1), altogether corroborating five of the ubiquitinated residues reported by (Ma et al., 2020) and revealing five novel ones (Figure 1). Thus, BIK1 is ubiquitinated on multiple surface-exposed lysines *in vivo*: three in the N-terminal variable domain (K31, K41, K61), seven in the canonical kinase domain (K95, K106, K155, K170, K186, K286, K337), and five in the C-terminal region (K358, K366, K369, K374, K388) (Figure 1). Whether RHA3A/B and PUB25/26 compete for these sites or ubiquitinate distinct lysines remains to be tested experimentally, as does clarifying which E2 conjugating enzymes work with respective E3 ligases to catalyze these events (Turek et al., 2018). Furthermore, as the phospho-status of BIK1 has been shown to affect its regulation by both RHA3A/B and PUB25/26 (Wang et al., 2018; Ma et al., 2020), another challenge will be resolving the biochemical mechanisms underlying this interplay.

Analysis of gene ontology (GO) terms associated with proteins identified in the high-confidence dataset (Table S1) indicated an enrichment of proteins localized to the ‘plasma membrane’ (p=1.53 x10^{-114}) (Table S3). Because we analysed the samples in the mass spectrometer in data-dependent mode, without quantification, we are unable to comment on differences between genotypes or immune treatments. Therefore, any immune-triggered events must be corroborated experimentally. Multiple sequence alignments of peptides spanning -10 to +10 amino- and carboxyl-

bioRxiv preprint doi: https://doi.org/10.1101/2020.09.16.299883; this version posted September 17, 2020. The copyright holder for this preprint (which was not certified by peer review) is the author/funder, who has granted bioRxiv a license to display the preprint in perpetuity. It is made available under aCC-BY-NC-ND 4.0 International license.

terminal to the modified lysines indicated very little consensus and no significant motifs (Figure S2). Unlike other post-translational modifications, the ubiquitination reaction requires coordination between E1 activating, E2 conjugating, and E3 ligase enzymes (Vierstra, 2012). While it may be possible for individual E2-E3 pairs to exhibit residue-level specificity on their target proteins, data from multiple species suggests that surface-availability may be the only unifying feature of ubiquitinated residues (Danielsen et al., 2011).

We identified ubiquitinated peptides mapping to proteins from diverse families, including aquaporins, H^+ and Ca^{2+} ATPases, remorins, several classes of transporters, cellulose synthases, and others (Tables S1 and S2). Comparison between our dataset and 8 published Arabidopsis ubiquitome datasets, as well as manual inspection of the literature, revealed 265 novel ubiquitin targets (Table S4). We noted that molecular function GO terms ‘protein modification’ (p=1.79 x10^{-12}), ‘phosphorylation’ (p=2.15 x10^{-26}), and ‘response to stimulus’ (p=6.44 x10^{-21}) were particularly enriched in our dataset (Table S3). Interestingly, we identified multiple ubiquitinated lysines on over 70 RKs representing diverse subgroups, including FLS2, EFR, CERK1, LORE, RLK7, SOBIR1/EVR, LIK1, RKL1, WAK1, WAK2, FER, ER, BAM1, BAM2, and others (Table 1). We also identified ubiquitination sites on more than 20 plasma membrane-associated cytoplasmic protein kinases from several subgroups (Table 1). Because analysis of tryptic peptides with ubiquitinated lysine residues enriched by anti-K-ε-GG does not allow for discrimination between mono- or poly-ubiquitination, it is likely that we have captured both degradative and non-degradative ubiquitination on these protein kinases. Given the broad interest in phosphorylation-based signal transduction and protein homeostasis, we expect this

bioRxiv preprint doi: https://doi.org/10.1101/2020.09.16.299883; this version posted September 17, 2020. The copyright holder for this preprint (which was not certified by peer review) is the author/funder, who has granted bioRxiv a license to display the preprint in perpetuity. It is made available under aCC-BY-NC-ND 4.0 International license.

information will be valuable to the plant research community, and look forward to future studies that explore the function of these ubiquitination events.

Footnotes

Acknowledgements

We thank Jan Sklenar for helpful suggestions and technical assistance, and are grateful to Melissa Bredow for help using Phyre2 and PyMol. We thank Libo Shan and Ping He for sharing data prior to publication.

Funding

This research was funded through a Biotechnology and Biological Sciences Research Council (BBSRC) Anniversary Future Leader Fellowship (J.M.), a Natural Sciences and Engineering Research Council of Canada (NSERC) Discovery grant (J.M.), a John R. Evans Leader's Fund grant from the Canadian Foundation for Innovation and the Ontario Ministry of Research and Innovation (J.M.), Queen's University start-up funds (J.M.), a grant from the European Research Council under the Grant Agreement 309858 (grant "PHOSPHinnATE", C.Z.), and through generous support of the Gatsby Charitable Foundation (C.Z. and F.L.H.M). L.E.G. and K.D. were supported by NSERC Canada Graduate Scholarships for Masters students (CGS-M), NSERC Michael Smith Foreign Study Supplements, and Ontario Graduate Scholarships (OGS).

bioRxiv preprint doi: https://doi.org/10.1101/2020.09.16.299883; this version posted September 17, 2020. The copyright holder for this preprint (which was not certified by peer review) is the author/funder, who has granted bioRxiv a license to display the preprint in perpetuity. It is made available under aCC-BY-NC-ND 4.0 International license.

Author Contributions

F.L.H.M. and J.M. designed the research; L.E.G. and F.L.H.M. performed the experiments; L.E.G., P.D., K.D., F.L.H.M., and J.M. analyzed the data; C.Z., F.L.H.M., and J.M. supervised the work; J.M. wrote the letter with input from all authors.

References

Couto D, Niebergall R, Liang X, Bücherl CA, Sklenar J, Macho AP, Ntoukakis V, Derbyshire P, Altenbach D, Maclean D, et al (2016) The Arabidopsis Protein Phosphatase PP2C38 Negatively Regulates the Central Immune Kinase BIK1. PLoS Pathog **12**: e1005811

Couto D, Zipfel C (2016) Regulation of pattern recognition receptor signalling in plants. Nat Rev Immunol **16**: 537–552

Danielsen JMR, Sylvestersen KB, Bekker-Jensen S, Szklarczyk D, Poulsen JW, Horn H, Jensen LJ, Mailand N, Nielsen ML (2011) Mass spectrometric analysis of lysine ubiquitylation reveals promiscuity at site level. Mol Cell Proteomics **10**: M110.003590

Jiang Y, Han B, Zhang H, Mariappan KG, Bigeard J, Colcombet J, Hirt H (2019) MAP4K4 associates with BIK1 to regulate plant innate immunity. EMBO Rep. 20:

Kelley LA, Mezulis S, Yates CM, Wass MN, Sternberg MJE (2015) The Phyre2 web portal for protein modeling, prediction and analysis. Nat Protoc **10**: 845–858

Lal NK, Nagalakshmi U, Hurlburt NK, Flores R, Bak A, Sone P, Ma X, Song G, Walley J, Shan L, et al (2018) The Receptor-like Cytoplasmic Kinase BIK1 Localizes to the Nucleus and Regulates Defense Hormone Expression during Plant Innate Immunity. Cell Host Microbe **23**: 485–497.e5

Liang X, Zhou J-M (2018) Receptor-Like Cytoplasmic Kinases: Central Players in Plant Receptor Kinase-Mediated Signaling. Annu Rev Plant Biol **69**: 267–299

Ma X, Claus LAN, Leslie ME, Tao K, Wu Z, Liu J, Yu X, Li B, Zhou J, Savatin DV, et al (2020) Ligand-induced monoubiquitination of BIK1 regulates plant immunity. Nature **581**: 199–203

Mithoe SC, Menke FL (2018) Regulation of pattern recognition receptor signalling by phosphorylation and ubiquitination. Curr Opin Plant Biol **45**: 162–170

bioRxiv preprint doi: https://doi.org/10.1101/2020.09.16.299883; this version posted September 17, 2020. The copyright holder for this preprint (which was not certified by peer review) is the author/funder, who has granted bioRxiv a license to display the preprint in perpetuity. It is made available under aCC-BY-NC-ND 4.0 International license.

Monaghan J, Matschi S, Shorinola O, Rovenich H, Matei A, Segonzac C, Malinovsky FG, Rathjen JP, MacLean D, Romeis T, et al (2014) The calcium-dependent protein kinase CPK28 buffers plant immunity and regulates BIK1 turnover. Cell Host Microbe **16**: 605–615

Paez Valencia J, Goodman K, Otegui MS (2016) Endocytosis and Endosomal Trafficking in Plants. Annu Rev Plant Biol **67**: 309–335

Shiu S-H, Bleecker AB (2001) Plant Receptor-Like Kinase Gene Family: Diversity, Function, and Signaling. Science Signaling **2001**: re22–re22

Shiu SH, Bleecker AB (2003) Expansion of the receptor-like kinase/Pelle gene family and receptor-like proteins in Arabidopsis. Plant Physiol **132**: 530–543

Turek I, Tischer N, Lassig R, Trujillo M (2018) Multi-tiered pairing selectivity between E2 ubiquitin–conjugating enzymes and E3 ligases. J. Biol. Chem.

Udeshi ND, Mertins P, Svinkina T, Carr SA (2013) Large-scale identification of ubiquitination sites by mass spectrometry. Nat Protoc **8**: 1950–1960

Vierstra RD (2012) The expanding universe of ubiquitin and ubiquitin-like modifiers. Plant Physiol **160**: 2–14

Walton A, Stes E, Cybulski N, Van Bel M, Inigo S (2016) It's time for some "site"-seeing: novel tools to monitor the ubiquitin landscape in Arabidopsis thaliana. The Plant

Wang J, Grubb LE, Wang J, Liang X, Li L, Gao C, Ma M, Feng F, Li M, Li L, et al (2018) A Regulatory Module Controlling Homeostasis of a Plant Immune Kinase. Mol Cell **69**: 493–504.e6

Zhang M, Chiang Y-H, Toruño TY, Lee D, Ma M, Liang X, Lal NK, Lemos M, Lu Y-J, Ma S, et al (2018) The MAP4 Kinase SIK1 Ensures Robust Extracellular ROS Burst and Antibacterial Immunity in Plants. Cell Host Microbe **24**: 379–391.e5

Zipfel C, Kunze G, Chinchilla D, Caniard A, Jones JDG, Boller T, Felix G (2006) Perception of the bacterial PAMP EF-Tu by the receptor EFR restricts Agrobacterium-mediated transformation. Cell **125**: 749–760

bioRxiv preprint doi: https://doi.org/10.1101/2020.09.16.299883; this version posted September 17, 2020. The copyright holder for this preprint (which was not certified by peer review) is the author/funder, who has granted bioRxiv a license to display the preprint in perpetuity. It is made available under aCC-BY-NC-ND 4.0 International license.

Tables and Figures

Table 1: Ubiquitinated protein kinases identified in this study.

Proteins matching the gene ontology term "kinase activity" were filtered from Supplementary Tables S1 and S2 and classified based on phylogenies presented by (Shiu and Bleecker, 2001; Shiu and Bleecker, 2003). *Residues that are only supported by a single observation (Table S2) are indicated by an asterisk and should be interpreted with caution. **Residues that were observed only after manual inspection of mass spectra matching BIK1 are indicated with two asterisks and shown in Supplementary Figure S1.

Receptor-like protein kinases

Protein family	Accession	Protein name	K-GG
SD-1	AT1G11300	EGM1	K514, K527
	AT4G27300	SD1-1	K518*, K550*, K648
	AT4G21380	ARK3/RK3/SD1-8	K661
	AT1G11350	CBRLK1/RKS2	K528
	AT1G61550	S-locus lectin protein kinase family protein	K507
	AT1G11330	RDA2	K529, K542
	AT1G61380	LORE/SD1-29	K493, K506*
SD-2	AT2G19130	S-locus lectin protein kinase family protein	K498*, K591
	AT1G34300	Lectin protein kinase family protein	K489*, K710
	AT4G32300	SD2-5	K641*, K727
L-LEC	AT4G28350	LecRK-VII.2	K339
	AT3G53380	LecRK-VIII.1	K374
	AT2G37710	RLK/LecRK-IV.1	K350*, K370

bioRxiv preprint doi: https://doi.org/10.1101/2020.09.16.299883; this version posted September 17, 2020. The copyright holder for this preprint (which was not certified by peer review) is the author/funder, who has granted bioRxiv a license to display the preprint in perpetuity. It is made available under aCC-BY-NC-ND 4.0 International license.

C-LEC	AT1G52310	C-type lectin receptor kinase	K265*, K278*, K292
CRK/DUF26	AT1G70520	CRK2	K379*
	AT4G23180	CRK10/RLK4	K438*, K449
	AT4G23190	CRK11/RLK3	K349, K366, K368, K400*, K451
	AT4G23300	CRK22	K352, K369, K371, K381
	AT4G05200	CRK25	K448, K507
	AT4G11530	CRK34	K363, K399
	AT4G04570	CRK40	K376*, K402
URK-II	AT5G20050	URK-II family protein	K199*, K156
CrRLK1L-1	AT5G54380	THE1	K480*, K526, K534, K560*, K657*, K753*
	AT3G51550	FERONIA	K530, K534, K549, K561, K672, K759, K771, K773, K781*, K843*
	AT3G46290	HERK1	K479, K498, K501
	AT1G30570	HERK2	K518
	AT2G23200	CrRLK1L-1 family protein	K710
	AT5G38990	MDS1	K541, K554*, K646*
LRR-1	AT1G51800	IOS1	K721
	AT1G51890	LRR-Ia family protein	K543*
	AT2G37050	BSR050	K740
LRR-II	AT4G33430	SERK3/BAK1	K339*
	AT2G13800	SERK5/BAK8	K303
	AT5G10290	LRR-II family protein	K276, K314, K469
	AT5G16000	NIK1	K320*
	AT2G23950	CLERK	K317

bioRxiv preprint doi: https://doi.org/10.1101/2020.09.16.299883; this version posted September 17, 2020. The copyright holder for this preprint (which was not certified by peer review) is the author/funder, who has granted bioRxiv a license to display the preprint in perpetuity. It is made available under aCC-BY-NC-ND 4.0 International license.

LRR-III	AT3G17840	RLK902	K315, K336, K347
	AT1G48480	RKL1	K353, K506
	AT5G58300	LRR-III family protein	K326*
	AT2G26730	LRR-III family protein	K293, K315*, K416
	AT2G36570	PXC1	K319
	AT3G08680	LRR-III family protein	K407
	AT5G16590	LRR1	K317
STUBBELIG-receptor	AT1G53730	SRF6	K392*
	AT3G14350	SRF7	K322
	AT4G22130	SRF8	K344*, K353
LRR-VI	AT5G63410	LRR-VI family protein	K397, K427
	AT2G02780	LRR-VI family protein	K403*
LRR-VII	AT3G28040	LRR-VIIa family protein	K742, K728
	AT1G80870	LRR-VIIa family protein	K89
LRR-VIII	AT5G49760	HPCA	K600*, K605, K625, K685*
	AT3G14840	LIK1	K666, K677, K688*, K700, K774, K793, K808, K821, K963*
LRR-IX	AT1G66150	TMK1	K640, K746
	AT2G01820	TMK3	K601, K637*, K743, K812
	AT3G23750	BARK1	K736*
LRR-X	AT5G48380	BIR1	K354, K562
	AT3G28450	BIR2	K290, K514
LRR-V	AT5G42440	LRR-Xb family protein	K109
	AT2G01820	PSKR1	K757*
LRR-XI	AT5G65700	BAM1	K785

bioRxiv preprint doi: https://doi.org/10.1101/2020.09.16.299883; this version posted September 17, 2020. The copyright holder for this preprint (which was not certified by peer review) is the author/funder, who has granted bioRxiv a license to display the preprint in perpetuity. It is made available under aCC-BY-NC-ND 4.0 International license.

	AT3G49670	BAM2	K781, K914
	AT1G28440	HSL1	K845, K957*
	AT1G09970	RLK7/LRR XI-23	K689, K703*, K818, K904, K966*
	AT2G33170	LRR XI family protein	K835*
	AT5G25930	LRR XI family protein	K701*, K941*
	AT1G72180	LRR XI family protein	K704*
LRR-XII	AT5G20480	EFR	K999, K1004
	AT5G46330	FLS2	K924, K940
LRR-XIII	AT1G27190	BIR3	K339
	AT1G31420	FEI1	K358
	AT4G08850	MIK2/BSR850	K770, K788, K793, K803, K818
	AT2G26330	ERECTA	K668
LRR-XV	AT3G02130	RPK2/TOAD2/CLI1	K1144
LRR-other	AT2G31880	SOBIR1/EVR	K640*
LysMa	AT3G21630	CERK1	K452
LRK10L-1a	AT1G25390	LRK10L4	K309
CRINKLY4-Like	AT5G46080	Protein kinase superfamily protein	K293
	AT3G55950	CCR3	K514
RKF3-Like	AT1G11050	Protein kinase superfamily protein	K449
WAK-Like	AT1G21250	WAK1/PRO25	K403, K425, K437
	AT1G21270	WAK2	K420, K432, K668*
	AT2G23450	WAKL family protein	K653*
Phototropin	AT3G45780	PHOT1/NPH1/RPT1	K526, K899

bioRxiv preprint doi: https://doi.org/10.1101/2020.09.16.299883; this version posted September 17, 2020. The copyright holder for this preprint (which was not certified by peer review) is the author/funder, who has granted bioRxiv a license to display the preprint in perpetuity. It is made available under aCC-BY-NC-ND 4.0 International license.

Cytoplasmic protein kinases

Protein family	Accession	Protein name	K-GG
RLCK-V	AT3G59110	RLCK-V family protein	K206
RLCK-VII	AT2G39660	BIK1	K31*,K41, K61, K155**, K337*, K358*, K366**, K369**, K374*, K388
	AT2G17220	PBL32/KIN3	K99, K242, K347
	AT5G13160	PBS1	K204
	AT5G18610	PBL27	K201
	AT5G03320	PBL40	K115*
RLCK-VIII	AT1G06700	PTI1-1	K71
	AT2G30740	PTI1-2	K38, K74
	AT3G59350	PTI1-3	K116, K133
	AT2G47060	PTI1-4	K46, K303*
	AT3G17410	PTI1-7/CARK1	K89, K190, K299
RLCK-XII	AT4G35230	BSK1	K85
	AT4G00710	BSK3	K67, K481*
	AT5G59010	BSK5	K64*
	AT3G54030	BSK6	K65
	AT1G63500	BSK7	K68*, K105, K304*
RLCK-XV	AT1G52540	RLCK-XV family protein	K249*
PERK	AT3G24550	PERK1	K303
	AT4G32710	PERK14	K18*
CDPK	AT3G20410	CPK9	K71, K115, K427
	AT4G04720	CPK21	K84, K526*
	AT5G66210	CPK28	K25, K34, K48*, K97, K108, K206*, K217, K351, K401*,

bioRxiv preprint doi: https://doi.org/10.1101/2020.09.16.299883; this version posted September 17, 2020. The copyright holder for this preprint (which was not certified by peer review) is the author/funder, who has granted bioRxiv a license to display the preprint in perpetuity. It is made available under aCC-BY-NC-ND 4.0 International license.

			K785
MAPK	AT3G63260	MRK1/RAF48	K342
Other protein kinase	AT1G65950	Protein kinase superfamily protein	K421
	AT4G00300	Fringe-related protein	K775
	AT1G56145	LRR transmembrane protein kinase	K725
	AT3G27560	ATN1	K44*
	AT1G03740	Protein kinase superfamily protein	K56*
	AT3G25840	PRP4KA	K462*
	AT4G35500	Protein kinase superfamily protein	K247*
	AT5G05200	Protein kinase superfamily protein	K31*
	AT5G40540	Protein kinase superfamily protein	K44*
	AT5G38480	GRF3/RCI1	K52
Other kinase	AT1G12000	Phosphofructokinase family protein	K23
	AT4G21534	SPHK2	K49, K59
	AT4G09320	NDPK1	K106
	AT5G50780	AtMORC4	K736*, K766
	AT1G12330	Cyclin-dependent kinase-like protein	K184
	AT4G36080	Inositol or phosphatidylinositol kinase	K3581*
	AT1G20930	CDKB2;2	K88*
	AT5G26667	PYR6	K54*
	AT4G29130	GIN2/HXK1	K117*
	AT1G10900	Phosphatidylinositol-4-phosphate 5-kinase family protein	K28*

228

bioRxiv preprint doi: https://doi.org/10.1101/2020.09.16.299883; this version posted September 17, 2020. The copyright holder for this preprint (which was not certified by peer review) is the author/funder, who has granted bioRxiv a license to display the preprint in perpetuity. It is made available under aCC-BY-NC-ND 4.0 International license.

bioRxiv preprint doi: https://doi.org/10.1101/2020.09.16.299883; this version posted September 17, 2020. The copyright holder for this preprint (which was not certified by peer review) is the author/funder, who has granted bioRxiv a license to display the preprint in perpetuity. It is made available under aCC-BY-NC-ND 4.0 International license.

Figure 1: BIK1 is ubiquitinated on multiple lysines *in vivo.*

A comparison between this study and (Ma et al., 2020) indicates that BIK1 is ubiquitinated on three lysines at its amino (N) terminus, seven in its kinase domain, and five at its carboxyl (C) terminus. Ubiquitinated lysines identified in (Ma et al., 2020) are shown in green, those identified in this study are shown in blue, and residues identified in both studies are magenta. Although the structure of the BIK1 canonical kinase domain was recently solved (Lal et al., 2018), we modelled BIK1 in Phyre2 (Kelley et al., 2015) in order to include the disordered N- and C-terminal ends of the protein so that all of the identified sites could be shown in this surface representation of BIK1 in PyMol.

bioRxiv preprint doi: https://doi.org/10.1101/2020.09.16.299883; this version posted September 17, 2020. The copyright holder for this preprint (which was not certified by peer review) is the author/funder, who has granted bioRxiv a license to display the preprint in perpetuity. It is made available under aCC-BY-NC-ND 4.0 International license.

Supplemental Data

Grubb LE, Derbyshire P, Dunning K, Zipfel C, Menke FLH, and Monaghan J.

"Large-scale identification of ubiquitination sites on membrane-associated proteins in *Arabidopsis thaliana* seedlings"

bioRxiv preprint doi: https://doi.org/10.1101/2020.09.16.299883; this version posted September 17, 2020. The copyright holder for this preprint (which was not certified by peer review) is the author/funder, who has granted bioRxiv a license to display the preprint in perpetuity. It is made available under aCC-BY-NC-ND 4.0 International license.

Supplemental Methods

The plant genotypes used in this study have been previously described (Monaghan et al., 2014). Twenty mg of seed from each genotype was surface-sterilized using chlorine gas and stratified at 4°C in the dark for 2 days. Seed was then transferred to 250 mL Erlenmeyer flasks containing 50 mL 0.5X Murashige and Skoog (MS) media supplemented with 0.05% sucrose, and shaken at 100 rpm at ambient temperature with a 10h photoperiod for 8 days. Seedlings were incubated with 50 µM MG-132 (Sigma Aldrich, UK) for 1 h with shaking, and then vacuum infiltrated with water (mock) or 1 µM elf18 peptide (EZ Biolabs, USA) for 10 min. Samples were flash frozen and ground to a coarse powder with a mortar and pestle in liquid N_2, then homogenized in urea lysis buffer (8 M urea, 50 mM Tris-HCl pH 8.0, 150 mM NaCl, 1 mM EDTA, 1 mM P9599 protease inhibitor (Sigma Alrich), 1 mM phenylmethylsulfonyl fluoride (PMSF), 50 µM PR-619 (Sigma Aldrich)) using equal volume-to-tissue ratio in a Potter tube for 10 min at 1,000 rpm. An aliquot of 1 mL was removed and kept for quick analysis of elf18-induced MAPK activation by immunoblot as previously described (Monaghan et al., 2014) (data not shown). The remaining homogenate was centrifuged at 5,856 x *g* for 1 h at 4°C. The supernatant was transferred to a polycarbonate tube and centrifuged at 110,000 x *g* for 1 h at 4°C. The pellet was resuspended in 2 mL of lysis buffer with PMSF, and protein concentration was determined using the Bradford Assay according to the manufacturer’s instructions (BioRad). Three mg of protein in 2 mL lysis buffer was incubated with 5 mM Tris(2-carboxyethyl)phosphine (TCEP) at ambient temperature for 45 min. Iodoacetamide (10mM) was added, and samples were incubated in the

bioRxiv preprint doi: https://doi.org/10.1101/2020.09.16.299883; this version posted September 17, 2020. The copyright holder for this preprint (which was not certified by peer review) is the author/funder, who has granted bioRxiv a license to display the preprint in perpetuity. It is made available under aCC-BY-NC-ND 4.0 International license.

dark for 30 min at ambient temperature. Finally, samples were diluted to 10 mL in 50 mM Tris-HCl pH 8.0 and digested with 30 µg of trypsin (Pierce, UK) at 30°C overnight.

Following trypsin digestion, samples were acidified with aliquots of 50% trifluoroacetic acid (TFA) to pH 3.0. Precipitate was removed by centrifugation at 1,600 x *g*, and the peptides in the supernatant were purified using 2.5 mL C18 silica reversed-phase chromatography Sep-Pak columns (Waters). Prior to use, the columns were equilibrated sequentially with 1 column volume (CV) MeOH, then 1 CV activation buffer (80% acetonitrile (ACN), 0.1% TFA), and then 5 CV of wash buffer (2% ACN, 0.1% TFA). Sample was added to the column and allowed to drip by gravity flow, collected, and applied to the column a second time before application of 5 CV wash buffer. Trypsin-digested peptides were eluted in 2 CV elution buffer (40% ACN, 0.1% TFA) and lyophilized.

The PTMScan® Ubiquitin Remnant Motif K-ε-GG antibody (Cell Signaling Technologies, UK) was first crosslinked to the agarose beads by washing each tube 3 times with 1 mL of 100 mM sodium borate pH 9.0, with centrifugation at 2,000 x *g* between each wash. The beads were then resuspended in 20 mM dimethyl pimelimidate (DMP) crosslinker and 100 mM sodium borate, and incubated for 1 h at room temperature with end-over-end rotation. The beads were washed twice with 1 mL of 200 mM ethanolamine pH 8.0, resuspended in 200 mM ethanolamine, and incubated overnight at 4°C with end-over-end rotation.

Prior to immunoaffinity purification (IP), crosslinked beads were washed 3 times with 1.5 mL IAP buffer (50 mM MOPS pH 7.2, 10 mM sodium phosphate, 50 mM NaCl). Lyophilized peptide samples were resuspended in 1.5 mL IAP buffer,

bioRxiv preprint doi: https://doi.org/10.1101/2020.09.16.299883; this version posted September 17, 2020. The copyright holder for this preprint (which was not certified by peer review) is the author/funder, who has granted bioRxiv a license to display the preprint in perpetuity. It is made available under aCC-BY-NC-ND 4.0 International license.

sonicated for 10 min, and centrifuged at 16,000 x *g* for 5 min. A volume of 1,300 μL of peptide sample was added to 300 μL of K-ε-GG beads in IAP buffer, and the remaining 200 μL was reserved as 'input' sample. The IP was conducted for 2 h at 4°C with end-over-end rotation, followed by centrifugation for 1 min at 2,000 x *g.* The supernatant was kept as the 'unbound' sample to test the efficiency of di-Gly enrichment. Beads were washed twice with 1.5 mL IAP buffer, then 3 times with high performance liquid chromatography (HPLC) grade water prior to elution with 100 μL of 0.15% TFA, and centrifugation 1 min at 2,000 x *g*. The supernatant was kept as the 'elution' sample for analysis by LC-MS/MS.

Input, unbound, and elution samples were partially purified using C18 Micro-Spin Stagetips columns (The Nest Group Inc.). The samples were acidified with 50% TFA to a pH of 3.0, and the columns were placed in 2 mL microcentrifuge tubes and equilibrated by washing 3 times with 200 μL MeOH and centrifuged at 135 x *g* for 30 s between each wash. Equilibration continued with 3 washes of 200 μL equilibration buffer (80% ACN, 0.1% TFA) and centrifugation for 2 min at 185 x *g*, followed by washing 6 times with wash buffer (2% ACN, 0.1% TFA). Peptide solutions were loaded twice into the equilibrated columns and centrifuged for 4 min at 240 x *g*. Columns were then washed 6 times with Wash Buffer as above, followed by tandem elutions in 150 μL elution buffer (40% ACN, 0.1% TFA).

To prepare for mass spectrometry, the input, unbound, and eluted samples were dehydrated using vacuum centrifugation (SpeedVac), and then resuspended in 2% ACN and 0.1% Formic Acid (FA), followed by vortexing and sonication for 10 min prior to a final centrifugation at 10,000 xg for 10 min. Samples were then loaded into

bioRxiv preprint doi: https://doi.org/10.1101/2020.09.16.299883; this version posted September 17, 2020. The copyright holder for this preprint (which was not certified by peer review) is the author/funder, who has granted bioRxiv a license to display the preprint in perpetuity. It is made available under aCC-BY-NC-ND 4.0 International license.

a 96-well plate for analysis on an Orbitrap Fusion Mass Spectrometer (ThermoFisher).

LC-MS/MS analysis was performed as described in (Bender et al., 2017) with the following modifications. On the Orbitrap Fusion MS/MS spectra were triggered with data dependent acquisition method using ‘top 20’ and ‘most intense ion’ settings. Peak lists in Mascot generic file format (.mgf files) were generated from raw files by using the MSConvert package (Matrix Science). Peak lists were searched using Mascot server v.2.4.1 (Matrix Science) against TAIR database (version 10), a separate in-house constructs database, and an in-house contaminants database. Tryptic peptides with up to 2 possible mis-cleavages and charge states +2, +3, +4, were allowed in the search. The following modifications were included in the search: oxidized methionine, diGly on lysine as variable modification and carbamido-methylated cysteine as static modification. Data were searched with a monoisotopic precursor and fragment ions mass tolerance 10ppm and 0.6 Da respectively. Mascot results were combined in Scaffold v. 4 (Proteome Software) and exported in Excel (Microsoft Office).

bioRxiv preprint doi: https://doi.org/10.1101/2020.09.16.299883; this version posted September 17, 2020. The copyright holder for this preprint (which was not certified by peer review) is the author/funder, who has granted bioRxiv a license to display the preprint in perpetuity. It is made available under aCC-BY-NC-ND 4.0 International license.

Supplemental References

Bailey TL, Boden M, Buske FA, Frith M, Grant CE, Clementi L, Ren J, Li WW, Noble WS (2009) MEME SUITE: tools for motif discovery and searching. Nucleic Acids Res **37**: W202–8

Bender KW, Blackburn RK, Monaghan J, Derbyshire P, Menke FLH, Zipfel C, Goshe MB, Zielinski RE, Huber SC (2017) Autophosphorylation-based Calcium (Ca2+) Sensitivity Priming and Ca2+/Calmodulin Inhibition of Arabidopsis thaliana Ca2+-dependent Protein Kinase 28 (CPK28). J Biol Chem **292**: 3988–4002

Crooks GE, Hon G, Chandonia J-M, Brenner SE (2004) WebLogo: a sequence logo generator. Genome Res **14**: 1188–1190

Igawa T, Fujiwara M, Takahashi H, Sawasaki T, Endo Y, Seki M, Shinozaki K, Fukao Y, Yanagawa Y (2009) Isolation and identification of ubiquitin-related proteins from Arabidopsis seedlings. J Exp Bot **60**: 3067–3073

Johnson A, Vert G (2016) Unraveling K63 Polyubiquitination Networks by Sensor-Based Proteomics. Plant Physiol **171**: 1808–1820

Kim D-Y, Scalf M, Smith LM, Vierstra RD (2013) Advanced proteomic analyses yield a deep catalog of ubiquitylation targets in Arabidopsis. Plant Cell **25**: 1523–1540

Manzano C, Abraham Z, López-Torrejón G, Del Pozo JC (2008) Identification of ubiquitinated proteins in Arabidopsis. Plant Mol Biol **68**: 145–158

Maor R, Jones A, Nühse TS, Studholme DJ, Peck SC, Shirasu K (2007) Multidimensional protein identification technology (MudPIT) analysis of ubiquitinated proteins in plants. Mol Cell Proteomics **6**: 601–610

Raudvere U, Kolberg L, Kuzmin I, Arak T, Adler P, Peterson H, Vilo J (2019) g:Profiler: a web server for functional enrichment analysis and conversions of gene lists (2019 update). Nucleic Acids Res **47**: W191–W198

Romero-Barrios N, Monachello D, Dolde U, Wong A, San Clemente H, Cayrel A, Johnson A, Lurin C, Vert G (2020) Advanced Cataloging of Lysine-63 Polyubiquitin Networks by Genomic, Interactome, and Sensor-Based Proteomic Analyses. Plant Cell **32**: 123–138

Svozil J, Hirsch-Hoffmann M, Dudler R, Gruissem W, Baerenfaller K (2014) Protein abundance changes and ubiquitylation targets identified after inhibition of the proteasome with syringolin A. Mol Cell Proteomics **13**: 1523–1536

Walton A, Stes E, Cybulski N, Van Bel M, Inigo S (2016) It's time for some "site"-seeing: novel tools to monitor the ubiquitin landscape in Arabidopsis thaliana. The Plant

bioRxiv preprint doi: https://doi.org/10.1101/2020.09.16.299883; this version posted September 17, 2020. The copyright holder for this preprint (which was not certified by peer review) is the author/funder, who has granted bioRxiv a license to display the preprint in perpetuity. It is made available under aCC-BY-NC-ND 4.0 International license.

Supplemental Tables

Table S1: High-confidence peptides identified in multiple experiments.

Peptides shown were filtered for the ubiquitin remnant diGly and were observed at least twice with a minimal Mascot score of 20. The peptide level false discovery rate was 0.025. Columns J to AR report the number of spectra observed in total (J), subtotals per genotype and treatment (K-Q) or in individual samples (S-AR). Column I shows whether the assignment of the diGly modified residue is possibly ambiguous (P) or not ambiguous (N).

Table S2: Peptides identified in single experiments.

Peptides shown were filtered for the ubiquitin remnant diGly and were observed at once with a minimal Mascot score of 20. The peptide level false discovery rate was 0.025. Columns J to AR report the number of spectra observed in total (J), subtotals per genotype and treatment (K-Q) or in individual samples (S-AR). Column I shows whether the assignment of the diGly modified residue is possibly ambiguous (P) or not ambiguous (N).

Table S3: Gene ontology terms associated with proteins identified in this study.

Gene ontology profiling was conducted using unique protein identifiers from Table S1 in g:profiler (Raudvere et al., 2019).

bioRxiv preprint doi: https://doi.org/10.1101/2020.09.16.299883; this version posted September 17, 2020. The copyright holder for this preprint (which was not certified by peer review) is the author/funder, who has granted bioRxiv a license to display the preprint in perpetuity. It is made available under aCC-BY-NC-ND 4.0 International license.

Table S4: Comparative analysis reveals 268 unique ubiquitin targets identified in this study.

Ubiquitinated proteins identified from earlier large-scale studies (Maor et al., 2007; Manzano et al., 2008; Igawa et al., 2009; Kim et al., 2013; Svozil et al., 2014; Johnson and Vert, 2016; Walton et al., 2016; Romero-Barrios et al., 2020) were compared to those identified in this study (Table S1) using Microsoft Excel. Manual inspection of the literature revealed additional ubiquitinated proteins, as well as proteins predicted to be ubiquitinated.

bioRxiv preprint doi: https://doi.org/10.1101/2020.09.16.299883; this version posted September 17, 2020. The copyright holder for this preprint (which was not certified by peer review) is the author/funder, who has granted bioRxiv a license to display the preprint in perpetuity. It is made available under aCC-BY-NC-ND 4.0 International license.

Supplemental Figures

Figure S1: Ubiquitinated residues identified on BIK1.

Ten tryptic peptides mapping to BIK1 contain di-Gly remnants in different genotypes and treatments as outlined in (A); the modified Lys residue is coloured blue. Mass spectra for each peptide were extracted from Scaffold and shown in (B); B- and Y-ions are coloured in red and blue, respectively.

Figure S2: Consensus motif analysis of ubiquitinated lysines.

Non-redundant full-length protein sequences were retrieved from The Arabidopsis Information Resource (TAIR) and peptide sequences -10 and +10 amino- and carboxyl-terminal to the modified lysines were identified using the MID function in Microsoft Excel. These 21-amino-acid peptide sequences were analyzed using the MEME Suite v5.1.1 MoMo motif finder tool (Bailey et al., 2009), however no statistically significant ($p<0.05$) consensus motifs were identified. A multiple-sequence alignment of the peptide sequences surrounding the modified lysine was created using WebLogo (Crooks et al., 2004). Blue residues contain positively-charged R-groups (KHR); Black residues are negatively-charged (DE); Magenta residues are hydrophobic (AILMFWYV); Green residues are polar uncharged (STNQ); Yellow residues are special cases (CGP).

A

BIK1 peptide sequence	K-GG	pBIK1:BIK1-HA					
		Col-0		CPK28-OE		cpk28-1	
		mock	elf18	mock	elf18	mock	elf18
KSSSTVAAAQKTEGEILSSTPVK	K31		1				1
KSSSTVAAAQKTEGEILSSTPVK	K41		2				
SSSTVAAAQKTEGEILSSTPVK	K41	2	2	4		2	2
SFTFNELKLATR	K61	2	3	2	2	2	3
LLVYEFMQKGSLENHLFR	K155	1					
MASVAVQcLSFEPKSRPTMDQVVR	K337		1				
ALQQLQDNLGKPSQTNPVKDTK	K358	1	1				2
ALQQLQDNLGKPSQTNPVKDTK	K366	1	2			1	1
ALQQLQDNLGKPSQTNPVKDTKK	K366/K369		1				
LGFKTGTTK	K374					1	
FTQKPFGR	K388	1	4	1			3

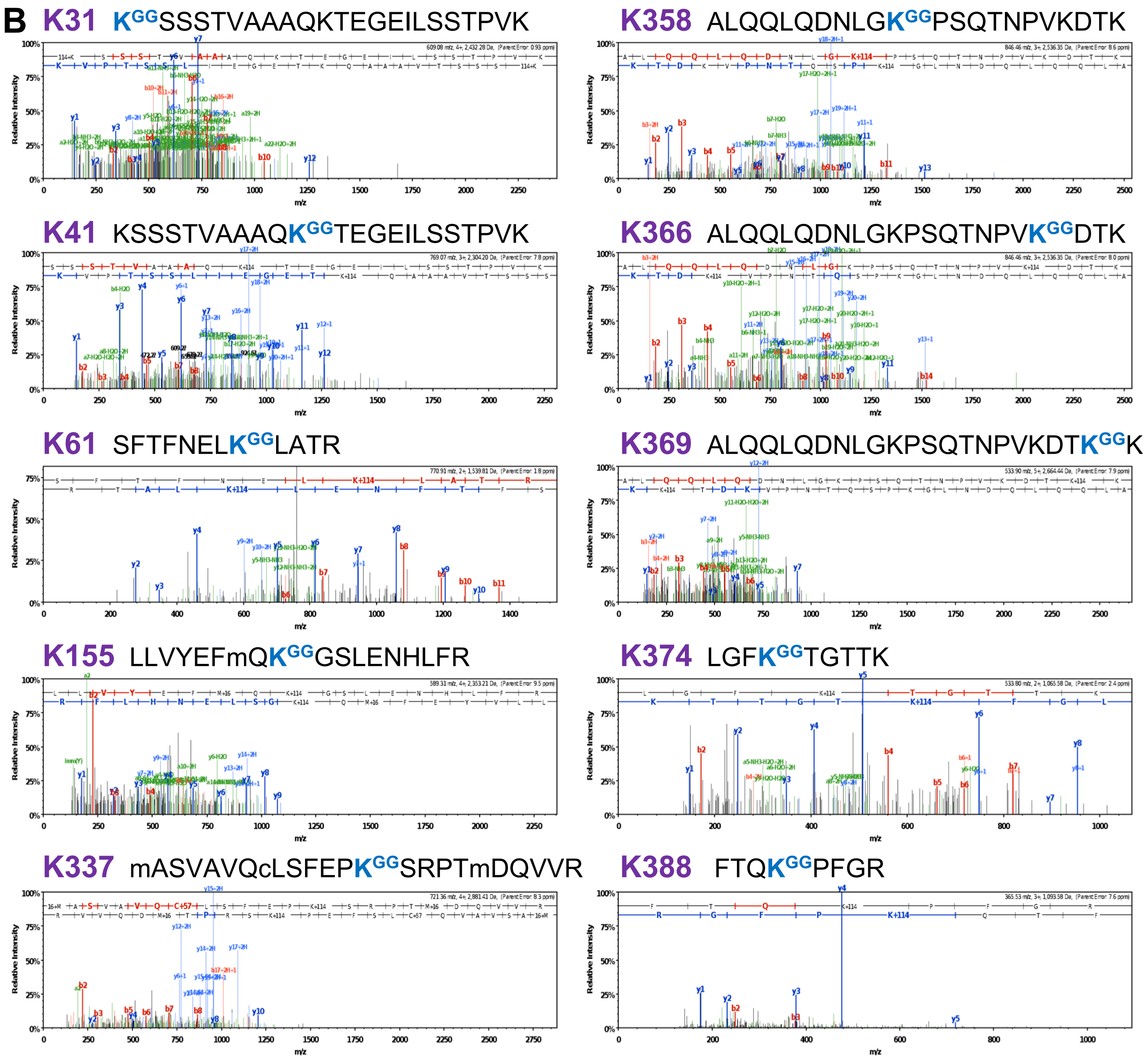

Figure S1: Ubiquitinated residues identified on BIK1.

Ten tryptic peptides mapping to BIK1 contain di-Gly remnants in different genotypes and treatments as outlined in (A); the modified Lys residue is coloured blue. Mass spectra for each peptide were extracted from Scaffold and shown in (B); B- and Y-ions are coloured in red and blue, respectively.

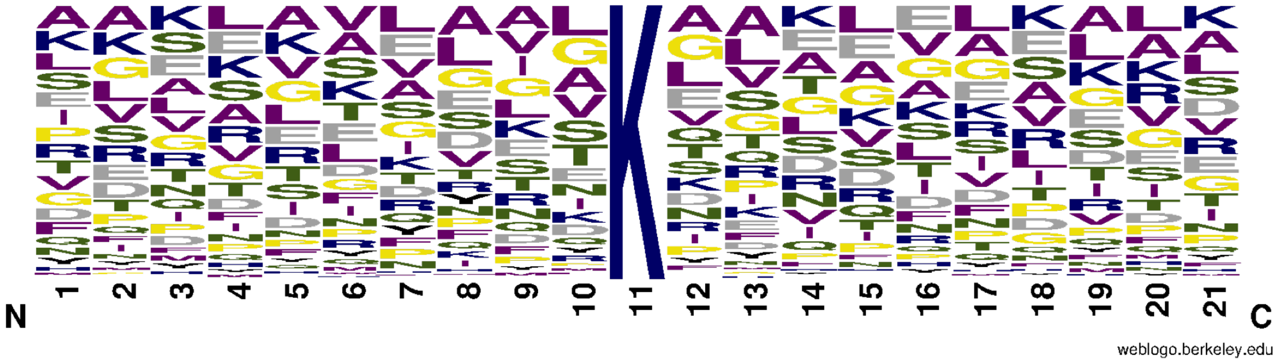

Figure S2: Consensus motif analysis of ubiquitinated lysines.

Non-redundant full-length protein sequences were retrieved from The Arabidopsis Information Resource (TAIR) and peptide sequences -10 and +10 amino- and carboxyl-terminal to the modified lysines were identified using the MID function in Microsoft Excel. These 21-amino-acid peptide sequences were analyzed using the MEME Suite v5.1.1 MoMo motif finder tool (Bailey et al., 2009), however no statistically significant ($p<0.05$) consensus motifs were identified. A multiple-sequence alignment of the peptide sequences surrounding the modified lysine was created using WebLogo (Crooks et al., 2004). Blue residues contain positively-charged R-groups (KHR); Black residues are negatively-charged (DE); Magenta residues are hydrophobic (AILMFWYV); Green residues are polar uncharged (STNQ); Yellow residues are special cases (CGP).

Table S4. Comparative analysis reveals 265 unique ubiquitin targets identified in this study.

Ubiquitinated proteins identified from earlier large-scale studies (Maor et al., 2007; Manzano et al., 2008; Igawa et al., 2009; Kim et al., 2013; Svozil et al., 2014; Johnson and Vert, 2016; Walton et al., 2016; Romero-Barrios et al., 2020) were compared to those identified in this study (Table S1) using Microsoft Excel. Manual inspection of the literature revealed additional ubiquitinated proteins, as well as proteins predicted to be ubiquitinated.

Accession	Protein name	References
AT1G01610	GPAT4	(Svozil et al., 2015; Romero-Barrios et al., 2020)
AT1G02520	ABC11/MDR8/PGP11	(Kim et al., 2013; Johnson and Vert, 2016)
AT1G02780	Emb2386 | Ribosomal protein L19e family protein	(Svozil et al., 2014; Walton et al., 2016)
AT1G03760	Prefoldin chaperone subunit family protein	(Walton et al., 2016)
AT1G04410	c-NAD-MDH1	(Saracco et al., 2009; Romero-Barrios et al., 2020)
AT1G04750	VAMP7B/VAMP721	(Saracco et al., 2009; Yun et al., 2013; Walton et al., 2016)
AT1G04820	TUA4/TOR2	(Zhang et al., 2019; Romero-Barrios et al., 2020)
AT1G06700	PTI1-1	(Kim et al., 2013)
AT1G06890	UXT3	
AT1G09195	Metal-dependent phosphohydrolase	
AT1G09330	ECHIDNA	
AT1G09920	TRAF-type zinc finger-related	
AT1G09970	LRR XI-23/RLK7	
AT1G10630	ARFA1F	(Aguilar-Hernández et al., 2017; Romero-Barrios et al., 2020)
AT1G11050	Protein kinase superfamily protein	
AT1G11260	STP1	(Romero-Barrios et al., 2020)
AT1G11300	EGM1	
AT1G11330	RDA2	

AT1G11350	CBRLK1/RKS2	
AT1G12000	Phosphofructokinase family protein	(Kim et al., 2013; Walton et al., 2016)
AT1G12110	NRT1.1/CHL1-1	(Johnson and Vert, 2016; Liu et al., 2017)
AT1G12330	Cyclin-dependent kinase-like protein	
AT1G12760	Zinc finger, C3HC4 type (RING finger) family protein	(Stone et al., 2005)
AT1G13210	ACA.l	
AT1G14200	RING/U-box superfamily protein	
AT1G14910	ENTH/ANTH/VHS superfamily protein	
AT1G15210	PDR7/ABCG35	(Kim et al., 2013)
AT1G15690	AVP1	(Kim et al., 2013; Johnson and Vert, 2016; Pizzio et al., 2017; Romero-Barrios et al., 2020)
AT1G16410	CYP79F1/BUS1/SPS1	
AT1G16690	Enhancer of polycomb-like transcription factor protein	
AT1G16860	Ubiquitin-specific protease family C19-related protein	
AT1G17145	RING/U-box superfamily protein	
AT1G17200	Uncharacterised protein family (UPF0497)	
AT1G17500	ATPase E1-E2 type family protein	(Kim et al., 2013)
AT1G17620	Late embryogenesis abundant (LEA) hydroxyproline-rich glycoprotein family	
AT1G18470	Transmembrane Fragile-X-F-associated protein	
AT1G19670	CLH1/CORI1	
AT1G20260	ATPase, V1 complex, subunit B protein	(Johnson and Vert, 2016; Romero-Barrios et al., 2020)
AT1G20330	SMT2/CVP1/FRL1	
AT1G20696	HMGB3/NFD3/NFD03	(Saracco et al., 2009; Walton et al., 2016)

AT1G21250	WAK1/PRO25	(Till et al., 2019)
AT1G21270	WAK2	
AT1G22280	PAPP2C	
AT1G22500	ATL15	(Stone et al., 2005)
AT1G22710	SUC2/SUT1	(Romero-Barrios et al., 2020; Xu et al., 2020)
AT1G23080	PIN7	(Abas et al., 2006; Titapiwatanakun, 2008; Thomann et al., 2009; Titapiwatanakun and Murphy, 2009)
AT1G25390	LRK10L4	
AT1G26120	ICME-LIKE1	
AT1G27000	Protein of unknown function (DUF1664)	(Romero-Barrios et al., 2020)
AT1G27190	BIR3	
AT1G28440	HSL1	
AT1G30320	Remorin family protein	
AT1G30360	ERD4	(Johnson and Vert, 2016; Romero-Barrios et al., 2020)
AT1G30400	MRP1/EST1/ABCC1	(Johnson and Vert, 2016; Romero-Barrios et al., 2020)
AT1G30440	Phototropic-responsive NPH3 family protein	(Kim et al., 2013)
AT1G30570	HERK2	
AT1G31420	FEI1	
AT1G32050	SCAMP family protein	
AT1G32090	ERD4	
AT1G32400	TOM2A	(Walton et al., 2016)
AT1G34300	Lectin protein kinase family protein	
AT1G43790	TED6	
AT1G45201	TLL1	(Kim et al., 2013)

AT1G45688	unknown protein	
AT1G47290	AT3BETAHSD/D1	
AT1G47530	MATE efflux family protein	
AT1G48480	RKL1	(Romero-Barrios et al., 2020)
AT1G51500	CER5/D3/ABCG12/WBC12	
AT1G51570	Calcium-dependent lipid-binding (CaLB domain) plant phosphoribosyltransferase family protein	
AT1G51800	IOS1	
AT1G52310	C-type lectin receptor kinase	
AT1G52320	unknown protein	
AT1G52740	HTA9	(Sura et al., 2017; Gómez-Zambrano et al., 2019; Romero-Barrios et al., 2020)
AT1G53210	Sodium/calcium exchanger family protein / calcium-binding EF hand family protein	
AT1G53310	PPC1/PEPC1	(Uhrig et al., 2008; Kim et al., 2013)
AT1G53750	RPT1A	(Kim et al., 2013; Walton et al., 2016)
AT1G55060	UBQ12	
AT1G55350	DEK1	
AT1G55450	S-adenosyl-L-methionine-dependent methyltransferases superfamily protein	
AT1G56070	LOS1	(Walton et al., 2016; Romero-Barrios et al., 2020)
AT1G56145	LRR transmembrane protein kinase	
AT1G56630	Alpha/beta-Hydrolases superfamily protein	
AT1G58030	CAT2	
AT1G58380	XW6	(Kim et al., 2013)

AT1G59870	PEN3/PDR8/ABCG36	(Kim et al., 2013; Johnson and Vert, 2016; Romero-Barrios et al., 2020)
AT1G61380	LORE/SD1-29	
AT1G61550	S-locus lectin protein kinase family protein	
AT1G61550	Major Facilitator Superfamily with SPX (SYG1/Pho81/XPR1)	
AT1G63500	BSK7	(Li et al., 2019)
AT1G64340	Unknown protein	
AT1G64950	CYP89A5	
AT1G65350	UBQ13	(Johnson and Vert, 2016; Romero-Barrios et al., 2020)
AT1G65720	Unknown protein	
AT1G65930	cICDH	(Kim et al., 2013; Svozil et al., 2015)
AT1G65950	Protein kinase superfamily protein	
AT1G66150	TMK1	
AT1G68070	Zinc finger, C3HC4 type (RING finger) family protein	
AT1G68720	TADA	(Walton et al., 2016)
AT1G68820	Transmembrane Fragile-X-F-associated protein	
AT1G70410	BCA4	(Kim et al., 2013; Johnson and Vert, 2016; Romero-Barrios et al., 2020)
AT1G70670	Caleosin-related family protein	
AT1G70770	Protein of unknown function DUF2359	(Kim et al., 2013; Romero-Barrios et al., 2020)
AT1G70940	PIN3	(Abas et al., 2006; Titapiwatanakun, 2008; Thomann et al., 2009; Titapiwatanakun and Murphy, 2009).
AT1G71140	MATE efflux family protein	
AT1G71880	SUC1	(Xu et al., 2020)

AT1G72370	P40/AP40/RP40/RPSAA	(Kim et al., 2013; Walton et al., 2016)
AT1G72500	Unknown protein	
AT1G72910	Toll-Interleukin-Resistance (TIR) domain-containing protein	
AT1G73220	AtOCT1	
AT1G74050	Ribosomal protein L6 family protein	(Walton et al., 2016)
AT1G74520	HVA22A	
AT1G74720	QKY | C2 calcium/lipid-binding plant phosphoribosyltransferase family protein	
AT1G75500	WAT1	
AT1G75840	ARAC5/ATGP3/ROP4	
AT1G76390	PUB43	
AT1G76600	Unknown protein	
AT1G77210	STP14	
AT1G77660	Histone H3 K4-specific methyltransferase SET7/9 family protein	
AT1G78870	UBC35	
AT1G78900	VHA-A	(Kim et al., 2013; Romero-Barrios et al., 2020)
AT1G79410	AtOCT5	
AT1G80870	LRR-VIIa family protein kinase	
AT2G01470	STL2P/ATSEC12	
AT2G01735	RIE1	
AT2G01820	TMK3	
AT2G02040	PTR2-B/NTR1	
AT2G04350	LACS8	(Walton et al., 2016)

AT2G13610	ABC-2 type transporter family protein	
AT2G13800	SERK5/BAK8	
AT2G17220	PBL32/KIN3	
AT2G18960	AHA1	(Kim et al., 2013; Johnson and Vert, 2016; Romero-Barrios et al., 2020)
AT2G19110	HMA4	
AT2G19130	S-locus lectin protein kinase family protein	
AT2G19730	Ribosomal L28e protein family	(Kim et al., 2013; Svozil et al., 2014; Johnson and Vert, 2016; Walton et al., 2016)
AT2G19750	Ribosomal protein S30 family protein	
AT2G20140	AAA-type ATPase family protein	(Kim et al., 2013)
AT2G20230	Tetraspanin family protein	
AT2G20740	Tetraspanin family protein	
AT2G20990	SYTA	(Romero-Barrios et al., 2020)
AT2G21410	VHA-A2	
AT2G23200	CrRLK1L-1 family protein	
AT2G23950	CLERK	
AT2G25070	Protein phosphatase 2C family protein	
AT2G25270	Unknown protein	
AT2G25450	2-oxoglutarate (2OG) and Fe(II)-dependent oxygenase superfamily protein	(Kim et al., 2013; Svozil et al., 2015)
AT2G26070	RTE1 | Protein of unknown function (DUF778)	
AT2G26250	FDH/KCS10	(McNeilly et al., 2018; Romero-Barrios et al., 2020)
AT2G26300	GPA1	

AT2G26330	ERECTA	
AT2G26730	LRR-III family protein kinase	
AT2G26910	PDR4	
AT2G27350	OTU-like cysteine protease family protein	
AT2G27690	CYP94C1	
AT2G27810	ATNAT12	(Walton et al., 2016)
AT2G28070	ABC-2 type transporter family protein	
AT2G28120	Major facilitator superfamily protein	
AT2G28520	VHA-A1	
AT2G30230	unknown protein	
AT2G30490	C4H/CYP73A5/REF3	(Kim et al., 2013)
AT2G30520	RPT2	(Johnson and Vert, 2016)
AT2G30620	Winged-helix DNA-binding transcription factor family protein	
AT2G30740	PTI1-2	(Kim et al., 2013)
AT2G30750	CYP71A12	
AT2G30870	GSTF10/ERD13/GSTF4	(Romero-Barrios et al., 2020)
AT2G30930	Unknown protein	(Svozil et al., 2014)
AT2G32730	26S proteasome regulatory complex, non-ATPase subcomplex, Rpn2/Psmd1 subunit	(Kim et al., 2013)
AT2G35635	UBQ7	(Walton et al., 2016)
AT2G35720	OWL1	
AT2G36100	Uncharacterised protein family (UPF0497)	(Svozil et al., 2015)
AT2G36380	PDR6	(Johnson and Vert, 2016)
AT2G36570	PXC1	

AT2G36850	GSL08	
AT2G36910	PGP1/ABCB1	(Walton et al., 2016)
AT2G37040	PAL1	(Kim et al., 2013; Svozil et al., 2014)
AT2G37050	BSR050	(Romero-Barrios et al., 2020)
AT2G37110	PLAC8 family protein	
AT2G37170	PIP2B/PIP2;2	(Lee et al., 2009; Romero-Barrios et al., 2020)
AT2G37470	Histone superfamily protein	
AT2G37710	RLK/LECRK-IV.1	
AT2G38360	PRA1.B4	(Svozil et al., 2014)
AT2G38810	HTA8	(Sura et al., 2017; Gómez-Zambrano et al., 2019)
AT2G38940	ATPT2/PHT1;4	(Huang et al., 2013; Lin et al., 2013; Park et al., 2014)
AT2G39210	Major facilitator superfamily protein	
AT2G39660	BIK1	(Monaghan et al., 2014; Wang et al., 2018; Ma et al., 2020)
AT2G41560	ACA4	
AT2G41840	Ribosomal protein S5 family protein	(Kim et al., 2013; Svozil et al., 2014; Johnson and Vert, 2016)
AT2G42600	ATPPC2	(Saracco et al., 2009; Kim et al., 2013; Svozil et al., 2014)
AT2G45820	Remorin family protein	(Svozil et al., 2014; Johnson and Vert, 2016)
AT2G45960	PIP1B/PIP1;2	(Lee et al., 2009; Kim et al., 2013; Johnson and Vert, 2016; Romero-Barrios et al., 2020)
AT2G46800	ZAT/ATMTP1/ATCDF1	
AT2G47000	MDR4/PGP4/ABCB4	(Kim et al., 2013; Johnson and Vert, 2016; Romero-Barrios et al., 2020)
AT2G47060	PTI1-4	(Kim et al., 2013)

AT2G47110	UBQ6	
AT2G47240	CER8/LACS1	
AT2G47630	Alpha/beta-Hydrolases superfamily protein	
AT3G01290	SPFH/Band 7/PHB domain-containing membrane-associated protein family	(Johnson and Vert, 2016; Romero-Barrios et al., 2020)
AT3G01390	VMA10	(Walton et al., 2016)
AT3G01420	ALPHA-DOX1	(Johnson and Vert, 2016)
AT3G01570	Oleosin family protein	(Deruyffelaere et al., 2015; Kretzschmar et al., 2018)
AT3G01670	Unknown protein	
AT3G02130	RPK2/TOAD2/CLI1	
AT3G03050	CSLD3/KJK/ATCSLD3	(Gu et al., 2016)
AT3G03310	ATLCAT3	
AT3G04120	GAPC/GAPC-1	(Peralta et al., 2016)
AT3G04840	Ribosomal protein S3Ae	(Kim et al., 2013; Svozil et al., 2014; Walton et al., 2016)
AT3G05160	Major facilitator superfamily protein	
AT3G05165	Major facilitator superfamily protein	
AT3G05200	ATL6	
AT3G05800	AIF1	
AT3G06330	RING/U-box superfamily protein	
AT3G06450	HCO3- transporter family	
AT3G08510	ATPLC2	(Pokotylo et al., 2014; Romero-Barrios et al., 2020)
AT3G08680	LRR-III family protein kinase	
AT3G08710	ATH9/TRX	
AT3G08930	LMBR1-like membrane protein	

AT3G09440	Heat shock protein 70 (Hsp 70) family protein	(Walton et al., 2016; Romero-Barrios et al., 2020)
AT3G09740	SYP71	(Walton et al., 2016; Romero-Barrios et al., 2020)
AT3G09840	CDC48,/CDC48A	(Kim et al., 2013; Walton et al., 2016)
AT3G11820	SYP121/PEN1	
AT3G11930	Adenine nucleotide alpha hydrolases-like superfamily protein	(Romero-Barrios et al., 2020)
AT3G12120	FAD2	(Dar et al., 2017)
AT3G14350	SRF7	
AT3G14690	CYP72A15	
AT3G14840	LIK1	(Kim et al., 2013)
AT3G14940	ATPPC3	(Kim et al., 2013)
AT3G15580	ATG8I/APG8H	
AT3G16180	Major facilitator superfamily protein	
AT3G17410	PTI1-7/CARK1	(Kim et al., 2013)
AT3G17650	YSL5/PDE321	
AT3G17840	RLK902	
AT3G17970	TOC64-III	(Ling et al., 2012)
AT3G18820	ATRABG3F/ATRAB7B/RAB71	
AT3G19450	CAD4/CAD-C	(Kim et al., 2013; Svozil et al., 2014)
AT3G19930	STP4	
AT3G20410	CPK9	
AT3G20660	AtOCT4	
AT3G21530	DNAse I-like superfamily protein	
AT3G21630	CERK1	(Yamaguchi et al., 2017)
AT3G23560	ALF5	

AT3G23820	GAE6	
AT3G24550	PERK1	(Kim et al., 2013)
AT3G25610	ATPase E1-E2 type family protein	
AT3G26830	PAD3/CYP71B15	
AT3G27390	unknown protein	
AT3G28040	LRR-VIIa family protein kinase	
AT3G28450	BIR2	
AT3G28860	ATMDR1/ATMDR11/PGP19/ABCB19	(Romero-Barrios et al., 2020)
AT3G42050	vacuolar ATP synthase subunit H family protein	(Kim et al., 2013; Johnson and Vert, 2016)
AT3G45600	TET3	
AT3G45780	PHOT1/NPH1/RPT1	(Deng et al., 2014)
AT3G46060	ARA3/RAB8A	
AT3G46290	HERK1	
AT3G46620	Zinc finger (C3HC4-type RING finger) family protein	
AT3G47250	Plant protein of unknown function (DUF247)	
AT3G48740	SWEET11	(Johnson and Vert, 2016; Romero-Barrios et al., 2020)
AT3G48890	ATMP2/ATMAPR3	(Kao et al., 2012; Svozil et al., 2014)
AT3G48990	AMP-dependent synthetase and ligase family protein	(Kim et al., 2013; Svozil et al., 2014; Walton et al., 2016)
AT3G49010	ATBBC1/RSU2	(Svozil et al., 2014; Walton et al., 2016)
AT3G49670	BAM2	
AT3G50480	HR4	
AT3G50930	BCS1	
AT3G51260	PAD1	(Svozil et al., 2014; Walton et al., 2016)
AT3G51460	RHD4	(Kim et al., 2013)

AT3G51550	FERONIA	(Kim et al., 2013; Guo et al., 2018)
AT3G52400	SYP122	(Johnson and Vert, 2016; Walton et al., 2016)
AT3G52920	Family of unknown function (DUF662)	(Walton et al., 2016)
AT3G52930	Aldolase superfamily protein	(Romero-Barrios et al., 2020)
AT3G53020	STV1/RPL24B/RPL24	(Kim et al., 2013; Walton et al., 2016)
AT3G53260	PAL2	(Saracco et al., 2009; Kim et al., 2013; Svozil et al., 2014)
AT3G53380	LecRK-VIII.1	
AT3G53420	PIP2A/PIP2;1	(Lee et al., 2009; Kim et al., 2013; Johnson and Vert, 2016; Romero-Barrios et al., 2020)
AT3G53480	PIS1/PDR9/ABCG37	(Johnson and Vert, 2016)
AT3G53780	ATRBL4	
AT3G53870	Ribosomal protein S3 family protein	(Saracco et al., 2009; Svozil et al., 2014; Romero-Barrios et al., 2020)
AT3G54030	BSK6	(Li et al., 2019)
AT3G54140	PTR1	
AT3G54300	VAMP727	
AT3G54560	HTA11	(Sura et al., 2017; Gómez-Zambrano et al., 2019)
AT3G55130	WBC19	
AT3G55360	CER10/ECR/TSC13	(Romero-Barrios et al., 2020)
AT3G55950	CCR3	
AT3G56170	CAN	
AT3G57330	ACA11	
AT3G57570	ARM repeat superfamily protein	

AT3G59110	RLCK-V family protein	
AT3G59350	Protein kinase superfamily protein	
AT3G60600	VAP27-1	
AT3G61180	RING/U-box superfamily protein	
AT3G61260	Remorin family protein	(Svozil et al., 2014; Walton et al., 2016)
AT3G62250	UBQ5	
AT3G62870	Ribosomal protein L7Ae/L30e/S12e/Gadd45 family protein	(Saracco et al., 2009; Kim et al., 2013; Svozil et al., 2014; Walton et al., 2016)
AT3G63260	MRK1/RAF48	(Benschop et al., 2007; Romero-Barrios et al., 2020)
AT4G00090	Transducin/WD40 repeat-like superfamily protein	(Kim et al., 2013)
AT4G00300	Fringe-related protein	
AT4G00360	CYP86A2/ATT1	
AT4G00710	BSK3	(Li et al., 2019)
AT4G01320	STE24	
AT4G01410	Late embryogenesis abundant (LEA) hydroxyproline-rich glycoprotein family	
AT4G02050	STP7	
AT4G02100	Heat shock protein DnaJ with tetratricopeptide repeat	
AT4G02230	Ribosomal protein L19e family protein	(Kim et al., 2013; Walton et al., 2016)
AT4G02700	SULTR3;2	
AT4G04340	ERD (early-responsive to dehydration stress) family protein	
AT4G04570	CRK40	
AT4G04720	CPK21	
AT4G05120	ENT3/FUR1/ATENT3	

AT4G05200	CRK25	(Johnson and Vert, 2016)
AT4G08850	MIK2/BSR850	
AT4G09320	NDPK1	(Walton et al., 2016)
AT4G11530	CRK34	
AT4G11680	Zinc finger, C3HC4 type (RING finger) family protein	
AT4G13770	CYP83A1/REF2	
AT4G13930	SHM4	(Zhou et al., 2012)
AT4G13940	HOG1/EMB1395/SAHH1/MEE58	(Walton et al., 2016; Aguilar-Hernández et al., 2017; Romero-Barrios et al., 2020)
AT4G14500	Polyketide cyclase/dehydrase and lipid transport superfamily protein	
AT4G14760	NET1B	
AT4G15610	Uncharacterised protein family (UPF0497)	
AT4G16370	OPT3	
AT4G16380	Heavy metal transport/detoxification superfamily protein	
AT4G16720	Ribosomal protein L23/L15e family protein	
AT4G17170	AT-RAB2/ATRABB1C	(Kim et al., 2013)
AT4G21380	ARK3/RK3/SD1-8	
AT4G21534	SPHK2	
AT4G22130	SRF8	
AT4G22690	CYP706A1	(Kim et al., 2013)
AT4G23180	CRK10/RLK4	
AT4G23190	CRK11/RLK3	
AT4G23300	CRK22	

AT4G23640	TRH1/ATKT3/KUP4	
AT4G23700	CHX17	(Johnson and Vert, 2016)
AT4G24990	ATGP4/MUB3	
AT4G25140	OLEO1/OLE1	(Deruyffelaere et al., 2015)
AT4G26550	Got1/Sft2-like vesicle transport protein family	
AT4G27300	SD1-1	
AT4G27500	PPI1	(Svozil et al., 2014; Walton et al., 2016)
AT4G28270	RMA2	
AT4G28350	LecRK-VII.2	
AT4G29410	Ribosomal L28e protein family	(Svozil et al., 2014)
AT4G30190	AHA2	(Kim et al., 2013; Johnson and Vert, 2016; Walton et al., 2016; Romero-Barrios et al., 2020)
AT4G30210	AR2	
AT4G31130	Protein of unknown function (DUF1218)	
AT4G31480	Coatomer, beta subunit	(Kim et al., 2013; Svozil et al., 2014; Johnson and Vert, 2016; Romero-Barrios et al., 2020)
AT4G31500	CYP83B1/SUR2/RNT1/RED1/ATR4	
AT4G31570	Unknown protein	(Kim et al., 2013; Svozil et al., 2014)
AT4G31590	ATCSLC05/ATCSLC5	
AT4G32150	VAMP711	
AT4G32300	SD2-5	(Kim et al., 2013)
AT4G32410	CESA1/RSW1	(Taylor, 2007; Watanabe et al., 2018; Romero-Barrios et al., 2020)
AT4G33360	FLDH | NAD(P)-binding Rossmann-fold superfamily protein	(Kim et al., 2013; Svozil et al., 2014)

AT4G35230	BSK1	(Kim et al., 2013; Li et al., 2019)
AT4G35790	PLD-DELTA	
AT4G36670	Major facilitator superfamily protein	
AT4G37640	ACA2	
AT4G38520	Protein phosphatase 2C family protein	
AT4G38630	RPN10/MCB1/MBP1	(Walton et al., 2016)
AT4G39080	VHA-A3	(Kim et al., 2013; Johnson and Vert, 2016; Romero-Barrios et al., 2020)
AT4G39950	CYP79B2	
AT4G40030	Histone superfamily protein	
AT5G01410	PDX1/PDX1.3/RSR4	(Kim et al., 2013; Svozil et al., 2014; Johnson and Vert, 2016; Walton et al., 2016; Romero-Barrios et al., 2020)
AT5G01460	LMBR1-like membrane protein	
AT5G02500	HSC70-1/HSP70-1	(Johnson and Vert, 2016; Walton et al., 2016; Romero-Barrios et al., 2020)
AT5G02540	NAD(P)-binding Rossmann-fold superfamily protein	
AT5G02870	Ribosomal protein L4/L1 family	(Walton et al., 2016)
AT5G03760	ATCSLA09,/ATCSLA9/RAT4	
AT5G04320	Shugoshin C terminus	
AT5G04530	KCS19	
AT5G05170	CESA3/IXR1/ATH-B/CEV1	(Taylor, 2007; Johnson and Vert, 2016; Watanabe et al., 2018; Romero-Barrios et al., 2020)
AT5G06530	ABC-2 type transporter family protein	
AT5G07910	Leucine-rich repeat (LRR) family protein	
AT5G08080	SYP132	

AT5G10290	LRR-II family protein kinase	
AT5G10360	EMB3010/RPS6B	(Walton et al., 2016)
AT5G10420	MATE efflux family protein	
AT5G13160	PBS1	
AT5G13550	SULTR4;1	
AT5G15490	UDP-glucose 6-dehydrogenase family protein	(Kim et al., 2013)
AT5G16130	Ribosomal protein S7e family protein	(Svozil et al., 2014; Walton et al., 2016)
AT5G16130	Ribosomal protein S7e family protein	(Svozil et al., 2014; Walton et al., 2016)
AT5G16590	LRR1	(Johnson and Vert, 2016; Romero-Barrios et al., 2020)
AT5G16870	Peptidyl-tRNA hydrolase II (PTH2) family protein	
AT5G16880	Target of Myb protein 1	(Svozil et al., 2014)
AT5G16910	CSLD2	(Gu et al., 2016)
AT5G17770	CBR1/CBR	(Kim et al., 2013)
AT5G17920	ATCIMS/ATMETS/ATMS1	(Walton et al., 2016; Romero-Barrios et al., 2020)
AT5G18380	Ribosomal protein S5 domain 2-like superfamily protein	(Kim et al., 2013)
AT5G18610	PBL27	
AT5G19600	SULTR3;5	
AT5G20050	URK-II family protein	
AT5G20480	EFR	
AT5G20650	COPT5	(Svozil et al., 2014)
AT5G22140	FAD/NAD(P)-binding oxidoreductase family protein	
AT5G22740	ATCSLA02/ATCSLA2	
AT5G26850	Uncharacterized protein	
AT5G27350	SFP1	

AT5G27930	Protein phosphatase 2C family protein	
AT5G35200	ENTH/ANTH/VHS superfamily protein	
AT5G38480	GRF3/RCI1	(Sato et al., 2011; Kim et al., 2013; Johnson and Vert, 2016)
AT5G38895	RING/U-box superfamily protein	
AT5G38990	MDS1	
AT5G39040	ALS1/TAP2	
AT5G39320	UDP-glucose 6-dehydrogenase family protein	(Svozil et al., 2014)
AT5G39510	VTI11/ZIG/SGR4	(Walton et al., 2016)
AT5G40420	OLEO2/OLE2	(Deruyffelaere et al., 2015)
AT5G41520	RNA binding Plectin/S10 domain-containing protein	(Svozil et al., 2014)
AT5G42440	LRR-Xb family protein	
AT5G42980	ATTRX3/ATH3	
AT5G43350	ATPT1/PHT1;1	(Huang et al., 2013; Lin et al., 2013; Park et al., 2014; Johnson and Vert, 2016)
AT5G43360	PHT3/ATPT4/PHT1;3	(Huang et al., 2013; Lin et al., 2013; Park et al., 2014)
AT5G43860	CLH2	
AT5G44790	RAN1/HMA7	
AT5G46050	PTR3	
AT5G46080	Protein kinase superfamily protein	
AT5G46330	FLS2	(Lu et al., 2011)
AT5G46860	VAM3/SYP22/SGR3	
AT5G47020	Unknown protein	
AT5G47120	ATBI-1	
AT5G47200	ATRABD2B/ATRAB1A	

AT5G47910	RBOHD	(Walton et al., 2016; Lee et al., 2020)
AT5G48380	BIR1	
AT5G48810	ATB5-B/CB5-D	(Svozil et al., 2014)
AT5G49760	HPCA	
AT5G50780	AtMORC4	
AT5G52240	MSBP1/ATMP1/AtMAPR5	(Kao et al., 2012; Svozil et al., 2014)
AT5G52650	RNA binding Plectin/S10 domain-containing protein	(Svozil et al., 2014; Walton et al., 2016)
AT5G53050	alpha/beta-Hydrolases superfamily protein	
AT5G53560	ATB5-A/ATCB5-E	(Saracco et al., 2009; Walton et al., 2016)
AT5G54170	Polyketide cyclase/dehydrase and lipid transport superfamily protein	
AT5G54380	THE1	(Kim et al., 2013)
AT5G55160	SUMO2	
AT5G55630	KCO1/TPK1	
AT5G55990	CBL2	
AT5G56030	HSP81-2/ERD8/HSP90.2	(Kim et al., 2013; Aguilar-Hernández et al., 2017)
AT5G56500	TCP-1/cpn60 chaperonin family protein	
AT5G57090	PIN2/EIR1/WAV6/AGR1	(Abas et al., 2006; Titapiwatanakun, 2008; Thomann et al., 2009; Titapiwatanakun and Murphy, 2009)
AT5G57350	AHA3	(Kim et al., 2013; Walton et al., 2016; Romero-Barrios et al., 2020)
AT5G58970	UCP2	
AT5G59910	HTB4	(Bergmüller et al., 2007; Romero-Barrios et al., 2020)
AT5G61910	DCD (Development and Cell Death) domain protein	

AT5G62390	BAG7	(Kim et al., 2013; Walton et al., 2016; Romero-Barrios et al., 2020)
AT5G62520	SRO5	
AT5G62670	AHA11	(Kim et al., 2013; Romero-Barrios et al., 2020)
AT5G62680	Major facilitator superfamily protein	
AT5G62740	HIR1	(Johnson and Vert, 2016; Romero-Barrios et al., 2020)
AT5G63410	LRR-VI family protein kinase	
AT5G64120	Peroxidase superfamily protein	
AT5G64440	FAAH	
AT5G64740	CESA6/IXR2/E112/PRC1	(Taylor, 2007; Watanabe et al., 2018)
AT5G65660	Hydroxyproline-rich glycoprotein family protein	
AT5G65700	BAM1	
AT5G66210	CPK28	
AT5G66620	DAR6	

Supplemental Table S4 References

Abas L, Benjamins R, Malenica N, Paciorek T, Wiśniewska J, Moulinier-Anzola JC, Sieberer T, Friml J, Luschnig C (2006) Intracellular trafficking and proteolysis of the Arabidopsis auxin-efflux facilitator PIN2 are involved in root gravitropism. Nat Cell Biol **8**: 249–256

Aguilar-Hernández V, Kim D-Y, Stankey RJ, Scalf M, Smith LM, Vierstra RD (2017) Mass Spectrometric Analyses Reveal a Central Role for Ubiquitylation in Remodeling the Arabidopsis Proteome during Photomorphogenesis. Mol Plant **10**: 846–865

Benschop JJ, Mohammed S, O’Flaherty M, Heck AJR, Slijper M, Menke FLH (2007) Quantitative phosphoproteomics of early elicitor signaling in Arabidopsis. Mol Cell Proteomics **6**: 1198–1214

Bergmüller E, Gehrig PM, Gruissem W (2007) Characterization of post-translational modifications of histone H2B-variants isolated from Arabidopsis thaliana. J Proteome Res **6**: 3655–3668

Dar AA, Choudhury AR, Kancharla PK, Arumugam N (2017) The FAD2 Gene in Plants: Occurrence, Regulation, and Role. Front Plant Sci **8**: 1789

Deng Z, Oses-Prieto JA, Kutschera U, Tseng T-S, Hao L, Burlingame AL, Wang Z-Y, Briggs WR (2014) Blue light-induced proteomic changes in etiolated Arabidopsis seedlings. J Proteome Res **13**: 2524–2533

Deruyffelaere C, Bouchez I, Morin H, Guillot A, Miquel M, Froissard M, Chardot T, D’Andrea S (2015) Ubiquitin-Mediated Proteasomal Degradation of Oleosins is Involved in Oil Body Mobilization During Post-Germinative Seedling Growth in Arabidopsis. Plant Cell Physiol **56**: 1374–1387

Gómez-Zambrano Á, Merini W, Calonje M (2019) The repressive role of Arabidopsis H2A.Z in transcriptional regulation depends on AtBMI1 activity. Nature Communications. doi: 10.1038/s41467-019-10773-1

Gu F, Bringmann M, Combs J, Yang J, Bergmann D, Nielsen E (2016) The Arabidopsis CSLD5 functions in cell plate formation in a cell cycle dependent manner. The Plant Cell tpc.00203.2016

Guo H, Nolan TM, Song G, Liu S, Xie Z, Chen J, Schnable PS, Walley JW, Yin Y (2018) FERONIA Receptor Kinase Contributes to Plant Immunity by Suppressing Jasmonic Acid Signaling in Arabidopsis thaliana. Curr Biol **28**: 3316–3324.e6

Huang T-K, Han C-L, Lin S-I, Chen Y-J, Tsai Y-C, Chen Y-R, Chen J-W, Lin W-Y, Chen P-M, Liu T-Y, et al (2013) Identification of downstream components of ubiquitin-conjugating enzyme PHOSPHATE2 by quantitative membrane proteomics in Arabidopsis roots. Plant Cell **25**: 4044–4060

Igawa T, Fujiwara M, Takahashi H, Sawasaki T, Endo Y, Seki M, Shinozaki K, Fukao Y, Yanagawa Y (2009) Isolation and identification of ubiquitin-related proteins from Arabidopsis seedlings. J Exp Bot **60**: 3067–3073

Johnson A, Vert G (2016) Unraveling K63 Polyubiquitination Networks by Sensor-Based Proteomics. Plant Physiol **171**:

1808–1820

Kao A-L, Lin Y-H, Chen RP-Y, Huang Y-Y, Chen C-C, Yang C-C (2012) E3-independent ubiquitination of AtMAPR/MSBP1. Phytochemistry **78**: 7–19

Kim D-Y, Scalf M, Smith LM, Vierstra RD (2013) Advanced proteomic analyses yield a deep catalog of ubiquitylation targets in Arabidopsis. Plant Cell **25**: 1523–1540

Kretzschmar FK, Mengel LA, Müller AO, Schmitt K, Blersch KF, Valerius O, Braus GH, Ischebeck T (2018) PUX10 Is a Lipid Droplet-Localized Scaffold Protein That Interacts with CELL DIVISION CYCLE48 and Is Involved in the Degradation of Lipid Droplet Proteins. Plant Cell **30**: 2137–2160

Lee D, Lal NK, Lin Z-JD, Ma S, Liu J, Castro B, Toruño T, Dinesh-Kumar SP, Coaker G (2020) Regulation of reactive oxygen species during plant immunity through phosphorylation and ubiquitination of RBOHD. Nat Commun **11**: 1838

Lee HK, Cho SK, Son O, Xu Z, Hwang I, Kim WT (2009) Drought Stress-Induced Rma1H1, a RING Membrane-Anchor E3 Ubiquitin Ligase Homolog, Regulates Aquaporin Levels via Ubiquitination in Transgenic Arabidopsis Plants. The Plant Cell **21**: 622–641

Ling Q, Huang W, Baldwin A, Jarvis P (2012) Chloroplast biogenesis is regulated by direct action of the ubiquitin-proteasome system. Science **338**: 655–659

Lin W-Y, Huang T-K, Chiou T-J (2013) NITROGEN LIMITATION ADAPTATION, a Target of MicroRNA827, Mediates Degradation of Plasma Membrane–Localized Phosphate Transporters to Maintain Phosphate Homeostasis in Arabidopsis. The Plant Cell **25**: 4061–4074

Liu W, Sun Q, Wang K, Du Q, Li W-X (2017) Nitrogen Limitation Adaptation (NLA) is involved in source-to-sink remobilization of nitrate by mediating the degradation of NRT1.7 in Arabidopsis. New Phytologist **214**: 734–744

Li Z, Shen J, Liang J (2019) Genome-Wide Identification, Expression Profile, and Alternative Splicing Analysis of the Brassinosteroid-Signaling Kinase (BSK) Family Genes in Arabidopsis. Int J Mol Sci. doi: 10.3390/ijms20051138

Lu D, Lin W, Gao X, Wu S, Cheng C, Avila J, Heese A, Devarenne TP, He P, Shan L (2011) Direct ubiquitination of pattern recognition receptor FLS2 attenuates plant innate immunity. Science **332**: 1439–1442

Manzano C, Abraham Z, López-Torrejón G, Del Pozo JC (2008) Identification of ubiquitinated proteins in Arabidopsis. Plant Mol Biol **68**: 145–158

Maor R, Jones A, Nühse TS, Studholme DJ, Peck SC, Shirasu K (2007) Multidimensional protein identification technology (MudPIT) analysis of ubiquitinated proteins in plants. Mol Cell Proteomics **6**: 601–610

Ma X, Claus LAN, Leslie ME, Tao K, Wu Z, Liu J, Yu X, Li B, Zhou J, Savatin DV, et al (2020) Ligand-induced monoubiquitination of BIK1 regulates plant immunity. Nature **581**: 199–203

McNeilly D, Schofield A, Stone SL (2018) Degradation of the stress-responsive enzyme formate dehydrogenase by the RING-type E3 ligase Keep on Going and the ubiquitin 26S proteasome system. Plant Mol Biol **96**: 265–278

Monaghan J, Matschi S, Shorinola O, Rovenich H, Matei A, Segonzac C, Malinovsky FG, Rathjen JP, MacLean D, Romeis T, et al (2014) The calcium-dependent protein kinase CPK28 buffers plant immunity and regulates BIK1 turnover. Cell Host Microbe **16**: 605–615

Park BS, Seo JS, Chua N-H (2014) NITROGEN LIMITATION ADAPTATION recruits PHOSPHATE2 to target the phosphate transporter PT2 for degradation during the regulation of Arabidopsis phosphate homeostasis. Plant Cell **26**: 454–464

Peralta DA, Araya A, Busi MV, Gomez-Casati DF (2016) The E3 ubiquitin-ligase SEVEN IN ABSENTIA like 7 mono-ubiquitinates glyceraldehyde-3-phosphate dehydrogenase 1 isoform in vitro and is required for its nuclear localization in Arabidopsis thaliana. Int J Biochem Cell Biol **70**: 48–56

Pizzio GA, Hirschi KD, Gaxiola RA (2017) Conjecture Regarding Posttranslational Modifications to the Arabidopsis Type I Proton-Pumping Pyrophosphatase (AVP1). Front Plant Sci **8**: 1572

Pokotylo I, Kolesnikov Y, Kravets V, Zachowski A, Ruelland E (2014) Plant phosphoinositide-dependent phospholipases C: variations around a canonical theme. Biochimie **96**: 144–157

Romero-Barrios N, Monachello D, Dolde U, Wong A, San Clemente H, Cayrel A, Johnson A, Lurin C, Vert G (2020) Advanced Cataloging of Lysine-63 Polyubiquitin Networks by Genomic, Interactome, and Sensor-Based Proteomic Analyses.

Plant Cell **32**: 123–138

Saracco SA, Hansson M, Scalf M, Walker JM, Smith LM, Vierstra RD (2009) Tandem affinity purification and mass spectrometric analysis of ubiquitylated proteins in Arabidopsis. Plant J **59**: 344–358

Sato T, Maekawa S, Yasuda S, Domeki Y, Sueyoshi K, Fujiwara M, Fukao Y, Goto DB, Yamaguchi J (2011) Identification of 14-3-3 proteins as a target of ATL31 ubiquitin ligase, a regulator of the C/N response in Arabidopsis. The Plant Journal **68**: 137–146

Stone SL, Hauksdóttir H, Troy A, Herschleb J, Kraft E, Callis J (2005) Functional analysis of the RING-type ubiquitin ligase family of Arabidopsis. Plant Physiol **137**: 13–30

Sura W, Kabza M, Karlowski WM, Bieluszewski T, Kus-Slowinska M, Pawełoszek Ł, Sadowski J, Ziolkowski PA (2017) Dual Role of the Histone Variant H2A.Z in Transcriptional Regulation of Stress-Response Genes. Plant Cell **29**: 791–807

Svozil J, Gruissem W, Baerenfaller K (2015) Proteasome targeting of proteins in Arabidopsis leaf mesophyll, epidermal and vascular tissues. Front Plant Sci **6**: 376

Svozil J, Hirsch-Hoffmann M, Dudler R, Gruissem W, Baerenfaller K (2014) Protein abundance changes and ubiquitylation targets identified after inhibition of the proteasome with syringolin A. Mol Cell Proteomics **13**: 1523–1536

Taylor NG (2007) Identification of cellulose synthase AtCesA7 (IRX3) in vivo phosphorylation sites--a potential role in regulating protein degradation. Plant Mol Biol **64**: 161–171

Thomann A, Lechner E, Hansen M, Dumbliauskas E, Parmentier Y, Kieber J, Scheres B, Genschik P (2009) Arabidopsis CULLIN3 Genes Regulate Primary Root Growth and Patterning by Ethylene-Dependent and -Independent Mechanisms. PLoS Genetics **5**: e1000328

Till CJ, Vicente J, Zhang H, Oszvald M, Deery MJ, Pastor V, Lilley KS, Ray RV, Theodoulou FL, Holdsworth MJ (2019) The Arabidopsis thaliana N-recognin E3 ligase PROTEOLYSIS1 influences the immune response. Plant Direct **3**: e00194

Titapiwatanakun B (2008) The regulation of P-glycoprotein and PIN by their cellular environment. Purdue University

Titapiwatanakun B, Murphy AS (2009) Post-transcriptional regulation of auxin transport proteins: cellular trafficking, protein phosphorylation, protein maturation, ubiquitination, and membrane composition. J Exp Bot **60**: 1093–1107

Uhrig RG, She Y-M, Leach CA, Plaxton WC (2008) Regulatory monoubiquitination of phosphoenolpyruvate carboxylase in germinating castor oil seeds. J Biol Chem **283**: 29650–29657

Walton A, Stes E, Cybulski N, Van Bel M, Inigo S (2016) It’s time for some “site”-seeing: novel tools to monitor the ubiquitin landscape in Arabidopsis thaliana. The Plant

Wang J, Grubb LE, Wang J, Liang X, Li L, Gao C, Ma M, Feng F, Li M, Li L, et al (2018) A Regulatory Module Controlling Homeostasis of a Plant Immune Kinase. Mol Cell **69**: 493–504.e6

Watanabe Y, Schneider R, Barkwill S, Gonzales-Vigil E, Hill JL Jr, Samuels AL, Persson S, Mansfield SD (2018) Cellulose synthase complexes display distinct dynamic behaviors during xylem transdifferentiation. Proc Natl Acad Sci U S A **115**: E6366–E6374

Xu Q, Yin S, Ma Y, Song M, Song Y, Mu S, Li Y, Liu X, Ren Y, Gao C, et al (2020) Carbon export from leaves is controlled via ubiquitination and phosphorylation of sucrose transporter SUC2. Proc Natl Acad Sci U S A **117**: 6223–6230

Yamaguchi K, Mezaki H, Fujiwara M, Hara Y, Kawasaki T (2017) Arabidopsis ubiquitin ligase PUB12 interacts with and negatively regulates Chitin Elicitor Receptor Kinase 1 (CERK1). PLoS One **12**: e0188886

Yun HS, Kwaaitaal M, Kato N, Yi C, Park S, Sato MH, Schulze-Lefert P, Kwon C (2013) Requirement of vesicle-associated membrane protein 721 and 722 for sustained growth during immune responses in Arabidopsis. Mol Cells **35**: 481–488

Zhang N, Xu J, Liu X, Liang W, Xin M, Du J, Hu Z, Peng H, Guo W, Ni Z, et al (2019) Identification of HSP90C as a substrate of E3 ligase TaSAP5 through ubiquitylome profiling. Plant Sci **287**: 110170

Zhou H, Zhao J, Yang Y, Chen C, Liu Y, Jin X, Chen L, Li X, Deng XW, Schumaker KS, et al (2012) UBIQUITIN-SPECIFIC PROTEASE16 Modulates Salt Tolerance in Arabidopsis by Regulating Na /H Antiport Activity and Serine Hydroxymethyltransferase Stability. The Plant Cell **24**: 5106–5122